$CD11b^{+}Ly6G^{-}$ myeloid cells mediate mechanical inflammatory pain hypersensitivity

Nader Ghasemlou[a], Isaac M. Chiu[a,b], Jean-Pierre Julien[c], and Clifford J. Woolf[a,1]

[a]F. M. Kirby Neurobiology Center, Boston Children's Hospital & Harvard Medical School, Boston, MA 02115; [b]Department of Microbiology and Immunobiology, Harvard Medical School, Boston, MA 02115; and [c]Research Centre of Institut Universitaire en Santé Mentale de Québec and Department of Psychiatry and Neuroscience, Laval University, Quebec City, QC, Canada G1J 2G3

Edited by Ruslan Medzhitov, Yale University School of Medicine, New Haven, CT, and approved October 27, 2015 (received for review January 24, 2015)

Pain hypersensitivity at the site of inflammation as a result of chronic immune diseases, pathogenic infection, and tissue injury is a common medical condition. However, the specific contributions of the innate and adaptive immune system to the generation of pain during inflammation have not been systematically elucidated. We therefore set out to characterize the cellular and molecular immune response in two widely used preclinical models of inflammatory pain: (*i*) intraplantar injection of complete Freund's adjuvant (CFA) as a model of adjuvant- and pathogen-based inflammation and (*ii*) a plantar incisional wound as a model of tissue injury-based inflammation. Our findings reveal differences in temporal patterns of immune cell recruitment and activation states, cytokine production, and pain in these two models, with CFA causing a nonresolving granulomatous inflammatory response whereas tissue incision induced resolving immune and pain responses. These findings highlight the significant differences and potential clinical relevance of the incisional wound model compared with the CFA model. By using various cell-depletion strategies, we find that, whereas lymphocyte antigen 6 complex locus G (Ly)$6G^{+}CD11b^{+}$ neutrophils and T-cell receptor (TCR) β^{+} T cells do not contribute to the development of thermal or mechanical pain hypersensitivity in either model, proliferating $CD11b^{+}Ly6G^{-}$ myeloid cells were necessary for mechanical hypersensitivity during incisional pain, and, to a lesser extent, CFA-induced inflammation. However, inflammatory ($CCR2^{+}Ly6C^{hi}$) monocytes were not responsible for these effects. The finding that a population of proliferating $CD11b^{+}Ly6G^{-}$ myeloid cells contribute to mechanical inflammatory pain provides a potential cellular target for its treatment in wound inflammation.

pain | inflammation | cytokines | monocytes | macrophages

Inflammation is a critical component of an organism's protective response to tissue injury, pathogen invasion, and disease, comprising exudative and cellular components, including circulating and tissue-resident immune cells (leukocytes) and their repertoire of secreted mediators. However, the inflammatory response needs to be controlled with carefully balanced pro- and antiinflammatory elements and clearing of necrotic tissue and elimination of pathogens, promoting tissue repair and a return of tissue homeostasis. Pain is a cardinal feature of inflammation and is often referred to as inflammatory pain when the two symptoms occur together (1). The activation of nociceptive sensory neurons during inflammation serves the important role of alerting the organism to the presence of tissue injury/inflammation, with the associated pain hypersensitivity contributing to the avoidance of further damage until healing has occurred (2). However, dysregulation of inflammation or of its resolution can result in persistent inflammation and chronic pain.

Inflammatory pain is thought to be the consequence of nociceptor activation and sensitization by inflammatory mediators, contributing, respectively, to spontaneous pain and localized pain hypersensitivity (3). Factors that sensitize nociceptors include those secreted by infiltrating/activated leukocytes, such as cytokines/chemokines, growth factors, and lipids, and those released from damaged cells, such as ATP, H^{+}, and reactive compounds like hydroxynonenals (4–7). Despite the common assumption that immune cells are the major drivers of inflammatory pain, the exact cell types involved and their roles in different types of tissue inflammation have not yet been elucidated.

During acute inflammation, among the first cells recruited are neutrophils that release toxic mediators in an effort to contain the injury or infection (8). This is followed by the infiltration of monocytes to the affected site, as well as the local activation and proliferation of skin-resident myeloid cells [e.g., macrophages (Mø), dendritic cells, and Langerhans cells] that phagocytose debris and begin the active process of resolution of inflammation and tissue repair (9–11). These nonneutrophil myeloid cells make up a large part of the innate immune response. Cells of lymphoid origin are part of the adaptive immune response that present at later phases of inflammation, including antigen recognition by T cells and antibody production by B cells (12). Mechanical and thermal pain hypersensitivity typically occurs concomitantly with the acute phase of inflammation and resolves over time as inflammation subsides, suggesting that it reflects innate immune activation.

Despite there being many origins of inflammation, pain neurobiologists commonly view inflammatory pain as a unitary state: essentially, pain that occurs in the presence of inflammation. The most common models used to study inflammatory pain are intraplantar injections of various substances that elicit an inflammatory response [e.g., complete Freund's adjuvant (CFA), zymosan, or carrageenan] or of the products of immune cells (e.g., IL-1β or prostaglandins). Animal models of inflammatory pain include incisional wounds (for postsurgical pain), UV B irradiation (for sunburn), and

Significance

Inflammatory mediators can activate and sensitize nociceptors, specialized high-threshold nerve fibers that relay noxious signals to the spinal cord and brain to initiate pain. However, the contribution of specific immune cell types to pain in animal models of inflammation remains largely unknown. We therefore characterized the immune response in two widely used preclinical models of inflammatory pain: intraplantar injection of complete Freund's adjuvant and plantar incisional wound. Cell-depletion strategies investigated the contribution of neutrophils, myeloid cells (including monocytes and macrophages), and T cells to pain behavior outcomes. Our results show that these two models induced quite different inflammatory processes and that targeted elimination of a subpopulation of nonneutrophil myeloid cells blocked development of mechanical hypersensitivity following incisional wounds.

Author contributions: N.G., I.M.C., and C.J.W. designed research; N.G. and I.M.C. performed research; J.-P.J. contributed new reagents/analytic tools; N.G., I.M.C., and C.J.W. analyzed data; and N.G., I.M.C., and C.J.W. wrote the paper.

The authors declare no conflict of interest.

This article is a PNAS Direct Submission.

Data deposition: The data reported in this paper have been deposited in the Gene Expression Omnibus (GEO) database, www.ncbi.nlm.nih.gov/geo (accession no. GSE73667).

[1]To whom correspondence should be addressed. Email: clifford.woolf@childrens.harvard.edu.

This article contains supporting information online at www.pnas.org/lookup/suppl/doi:10.1073/pnas.1501372112/-/DCSupplemental.

chemically induced inflammation (for arthritis or inflammatory bowel diseases). These all produce intense localized inflammatory responses and pain-related behavior. However, the precise nature of the immune response likely differs considerably from model to model and may also differ in relevance to clinical settings. Furthermore, the nature (spontaneous or evoked, thermal or mechanical), extent, and duration of the pain also differs from one inflammatory condition to another.

Here, our goal was to determine the specific contribution of different immune cells to the generation and maintenance of pain in two distinct forms of acute inflammation commonly used as inflammatory pain models: intraplantar injection of CFA and plantar incisional wound. We first detailed the cellular and molecular immune responses in these models and then used cell-specific targeting strategies to identify the relative contribution of $CD11b^{+}Ly6G^{+}$ (lymphocyte antigen 6 complex, locus G) neutrophils, $CD11b^{+}Ly6G^{-}$ myeloid cells (primarily monocytes and skin-resident Mø), and T-cell receptor (TCR) β^{+} T cells to the pain-related hypersensitivity, revealing a major contribution of a subtype of Mø to mechanical hypersensitivity after sterile tissue injury.

Results

To define the specific immune mechanisms of pain, we chose two distinct models of inflammation. For our first model, we used intraplantar injection of CFA, which consists of a mixture of paraffin oil (85% vol/vol), mannide monooleate (15% vol/vol), and heat-killed *Mycobacteria tuberculosis* (1 mg/mL), and is an immunological adjuvant (13–15). Second, we chose a modified plantar incision (injury to the skin and underlying muscle) to model sterile tissue injury-based inflammation (16–18). Both of these models evoke strong pain-like behavior in rodents (17, 19), and are widely used for preclinical mechanism-based and pharmacological studies.

Mechanical and Thermal Hypersensitivity Differ Depending on Inflammatory Conditions. We first compared changes in mechanical and thermal sensitivity over time in both models by using standard behavioral tests: sensitivity of response to a noxious thermal stimulus was measured as the latency to withdrawal after applying radiant heat to the plantar surface of the hind paw (Hargreaves test) and static mechanical pain threshold measured as the force (in grams) needed to elicit a withdrawal in at least 5 of 10 stimulations by using von Frey monofilaments. Although both models of inflammation resulted in rapid and sustained thermal and mechanical hypersensitivity relative to their respective preinflammation controls, the extent of the hypersensitivity and temporal patterns of recovery showed differences. Maximal effects for thermal and mechanical hypersensitivity were observed for both models early after onset of inflammation (6–24 h). However, the degree of thermal (Fig. 1*A*) and mechanical (Fig. 1*B*) hypersensitivity after CFA injection was not nearly as pronounced as that after plantar incision (Fig. 1*C* and *D*). Both injury models showed progressive recovery of thermal sensitivity and reached baseline values 7 d after injury (Fig. 1 *A* and *C*). Mechanical hypersensitivity, on the contrary, did not recover to baseline levels at 14 d after CFA injection (Fig. 1*B*), whereas it had recovered by 7 d after the incisional wound (Fig. 1*D*).

Comparison of Histological Changes During Inflammatory Pain. The nature and extent of the tissue damage and immune response was assessed by using H&E staining (Fig. 2*A*). CFA injection was characterized by a rapid (≤6 h) infiltration of immune cells that formed a florid granuloma by 3 d, persisting until the last day examined (day 14). This pathological picture of granulomatous inflammation typically occurs when a foreign body cannot be cleared by the phagocytic response; granulomatous inflammation and pain is not common in clinical settings (20). We chose to stop our analysis at day 14 because of the potential for systemic vasculitic inflammation, producing polyarthritis and meningitis (21). The infiltrating immune cells after intraplantar CFA administration were found primarily at the interface of the epidermis and dermis, with few cells in the underlying hypodermis that includes the muscles and tendons of the hind paw. The epidermis was largely unaffected after CFA injection, but there was disruption of the dermal layer (made up primarily of fibroblasts) in the first 24 h after injection (Fig. 2*A*).

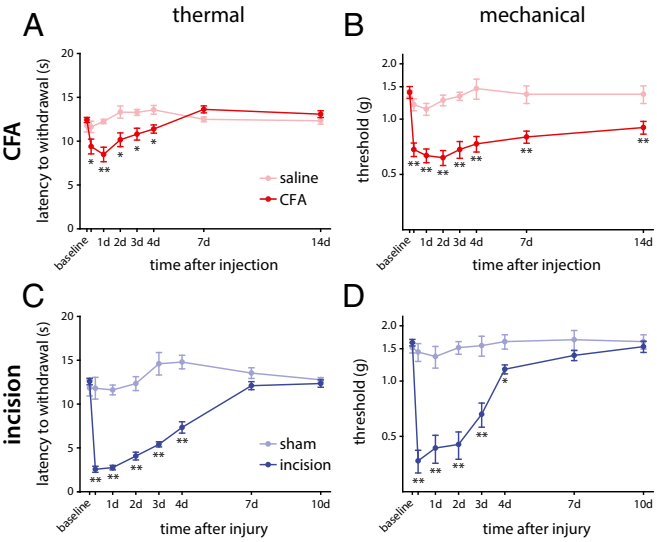

Fig. 1. Thermal and mechanical hypersensitivity after peripheral inflammation in C57BL/6J mice. (*A*) The latency of response to a radiant heat source (Hargreaves test) was assessed over time after intraplantar injection with CFA, with maximal effect relative to control saline injections 24 h after onset of inflammation that return to baseline levels by 7 d ($P < 0.001$, two-way RM-ANOVA). (*B*) The 50% response threshold to mechanical stimulation with von Frey monofilaments was reduced early after CFA injection and remained significantly decreased until 14 d ($P = 0.002$, two-way RM-ANOVA). (*C*) Thermal hypersensitivity after plantar incision had a maximal effect in the first 24 h after injury, returning to baseline by 7 d ($P < 0.001$, two-way RM-ANOVA), relative to sham injury. (*D*) Mechanical thresholds were similarly reduced after incision relative to sham injury, with maximal effect early after injury and returning to baseline by 7 d [$P < 0.001$, two-way RM-ANOVA; $*P < 0.05$ and $**P < 0.01$, two-way ANOVA with post hoc Tukey test; $n = 12$ (CFA), $n = 5$ (saline), $n = 10$ (incision), and $n = 6$ (sham)]. Time point not listed on graphs: 6 h. Graphs show mean ± SEM.

By contrast, histological analysis of the skin after plantar incision showed tissue damage across the epidermis, dermis, and hypodermis, and an infiltration of immune cells into these three layers within the first 6 h (Fig. 2*A*, *Right*). The presence of infiltrating cells following incision was greatest between 24 h and 3 d, with the cellular immune response largely resolved between 7 and 10 d. Wound closure was observed by 2–3 d, along with a characteristic thickening of the epidermis at the site of injury (22, 23). Some immune cells were still present within the dermal and, to a lesser extent, hypodermal layers 10 d after injury (the endpoint for incisional wounds). Thus, histological analysis indicates that CFA is characterized by a nonresolving granulomatous immune response whereas incisional wounds heal within 10 d of injury.

The Immune Response Is Distinct in Different Inflammatory Pain Conditions. We used flow cytometry to define the timing and percentage of myeloid and lymphoid cells following inflammation produced by the two models. Myeloid cells ($CD45^{+}CD11b^{+}$; Fig. 2*B*, black outline) made up the majority of infiltrating immune cells in both models, whereas lymphoid cells ($CD45^{+}CD11b^{-}$; Fig. 2*B*, red outline) made up fewer than 3% in each model and showed significant increases only beginning from day 7 in both models (Fig. 2 *B* and *C*). The increase in myeloid cells peaked at 24 h in both models. After CFA injection, myeloid cells

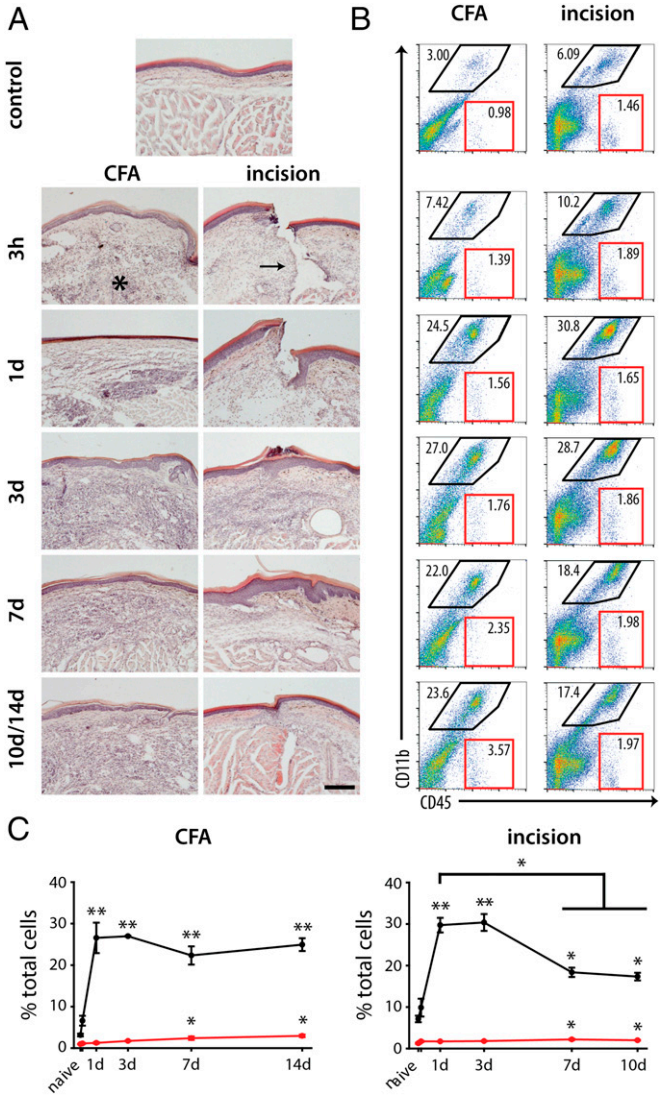

Fig. 2. The immune response after pathogenic inflammation and tissue injury results in disparate recruitment of immune cells and resolution. (*A*) The inflammatory response and its resolution were assessed in the skin using H&E staining. Naïve (control) skin is made up of a compact epidermal layer (the uppermost pink and blue layers), made primarily of keratinocytes and a dermal layer (a light pink layer) that is made of fibroblasts, adipocytes, and a matrix of collagen and elastin. Beneath these layers are the underlying muscles. CFA injection and incision result in the rapid (within 6 h) accumulation of immune cells at the site of injury. In the CFA model, the epidermal layer shows little change in structure whereas the underlying muscle layer is largely displaced by the infiltrating immune cells (asterisk), which does not resolve by 14 d. Incisional wounds (arrow) result in direct damage to the skin and muscle layers, which heal by 3 d, followed by resolution of the immune response, with most infiltrating cells absent by 10 d. (*B*) Flow cytometry shows myeloid (black outlines, $CD11b^{+}CD45^{+}$) and lymphoid (red outlines, $CD11b^{-}CD45^{+}$) cell recruitment into the hind paw after CFA injection and incisional wound over time. (*C*) Quantification of these two populations ($^{**}P < 0.001$ and $^{*}P < 0.05$, one-way RM-ANOVA vs. naïve) shows the sustained presence of myeloid cells after CFA injection but a reduction over time after incisional wound ($^{*}P < 0.05$, one-way RM-ANOVA, 7 and 14 d vs. 1 d). Lymphoid cells show increases only at later (>7 d) time points in both models of inflammation ($^{*}P < 0.05$; $n = 3$–4 per time point). Time point not listed on graphs: 3 h. Graphs show means ± SEM.

remained in the skin from 1 to 14 d at elevated levels, whereas there was a reduction of these cells over time after plantar incision ($P \leq 0.003$, one-way ANOVA for 1 d vs. 7 and 10 d postincision; Fig. 2*C*), although still well above baseline.

Subpopulations of immune cells were analyzed by flow cytometry using cell-specific markers. T cells ($CD45^{+}CD11b^{-}CD3^{+}$; Fig. 3*A*), neutrophils ($CD11b^{+}Ly6G^{+}$; Fig. 3*B*), and nonneutrophil myeloid cells ($CD11b^{+}Ly6G^{-}$; Fig. 3*C*) were profiled, with the cell-surface antigen Ly6C further used as a surrogate to assess myeloid cell activation states (Fig. S1 shows gating strategy). High expression of the Ly6C antigen ($Ly6C^{hi}$) is generally associated with a proinflammatory state and reduced expression ($Ly6C^{low}$) is indicative of an antiinflammatory or regenerative state (24, 25), while cells with intermediate expression of the receptor ($Ly6C^{med}$) are still poorly characterized but thought to show features intermediate between the $Ly6C^{hi}$ and $Ly6C^{low}$ cells (26). A small population of $Ly6C^{low}$ myeloid cells was present in naïve skin, likely made up of dendritic cells and other tissue-resident immune cells (27), whereas few neutrophils, $Ly6C^{hi}$ monocytes, or T cells were found in the uninjured hind paw (Fig. 3).

T cells (Fig. 3*A*, green gates) made up the smallest fraction of immune cells, increasing over time with the highest levels reached by 14 d. Neutrophil recruitment was rapid after intraplantar injection of CFA and incisional wound, showing significant increases from baseline at 3 h and peaking at 24 h in both inflammatory states (Fig. 3*B*). Although neutrophils were found in the skin after CFA injection for the duration of the study (14 d), they returned to baseline levels by 7 d after incision.

$CD11b^{+}Ly6G^{-}$ myeloid cells made up the majority of immune cells in the inflamed hind paw after CFA injection and the incisional wound from the 24-h time point onward. Differential Mø recruitment patterns occurred between the two models when $Ly6C^{low}$, $Ly6C^{med}$, and $Ly6C^{hi}$ expression were compared (Fig. 3*C*). Proinflammatory $Ly6C^{hi}$ monocytes (Fig. 3*C*, red gates) were the predominant immune cell population in the CFA-injected skin from 3 to 14 d, but, after incision, were present only at acute time points (days 1–3). There was an initial peak of $Ly6C^{med}$ and $Ly6C^{low}$Mø (Fig. 3*C*, purple and blue gates, respectively) at 24 h. Both these subsets decreased at 3 d, but remained elevated relative to naïve for the 14 d duration studied in the CFA-injected skin. The recruitment of $Ly6C^{med}$ and $Ly6C^{low}$ cells showed a different pattern after incisional wound (Fig. 3*D*): $Ly6C^{med}$ and $Ly6C^{hi}$ cells showed similar early and transient elevations, whereas the $Ly6C^{low}$ subset was the most abundant and persistent myeloid cell type in the skin after incisional wound from 3 d onward after injury (corresponding to the wound-healing phase). These data highlight the distinct cellular recruitment patterns and myeloid cell activation states present in these two inflammatory models (Fig. 3 *D* and *E*).

Cytokines and chemokines secreted by immune cells can change pain sensitivity, acting directly or indirectly on sensory neurons (28). We therefore used a multiplex cytokine assay to assess changes in the levels of these mediators in the two models. Of the 15 analytes examined, 11 were found to be significantly up-regulated in one or both models of inflammation (Fig. 4 and Table S1). The profiling of secreted mediators revealed major differences between the two models, likely because of the differential recruitment and activation of immune cells. Proinflammatory cytokines were most often up-regulated during the early phase of inflammation, whereas antiinflammatory cytokines and chemokines were more prominent in the later phase, when resolution of inflammation and tissue remodeling are occurring. Because of the differential recruitment patterns of immune cells and expression of cytokines/chemokines observed, we sought to identify the role of individual immune cell types in the generation and development of thermal and mechanical hypersensitivity in the two models. To do this, neutrophils, nonneutrophilic myeloid cells, and circulating T cells were selectively depleted and the impact of their depletion on pain sensitivity was assessed.

$TCR\beta^{+}$ T Cells Do Not Contribute to Inflammatory Pain. We tested the role of T cells in inflammatory pain by assaying the phenotype of T-cell–deficient $TCR\beta^{-/-}$ mice compared with WT littermate

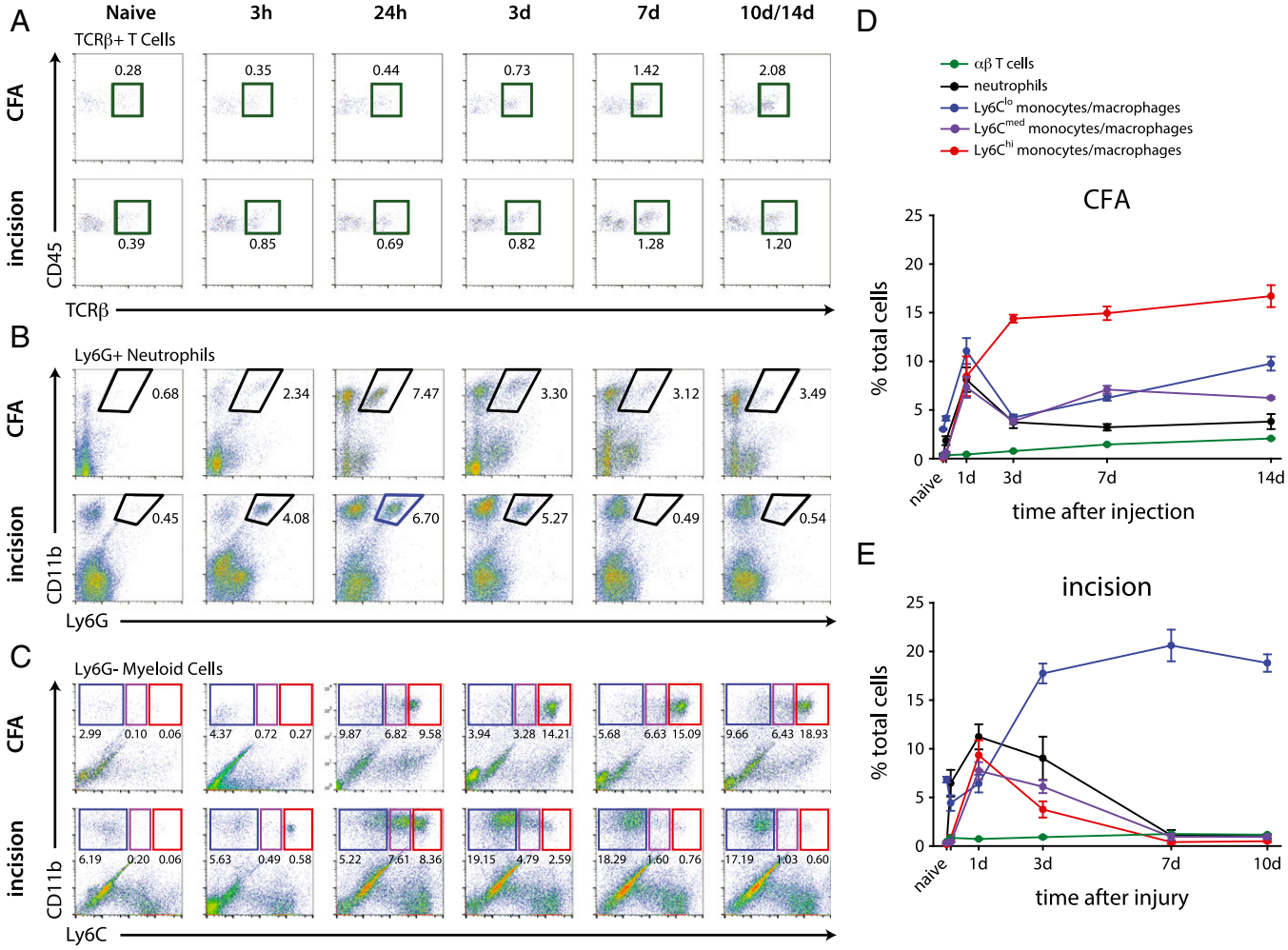

Fig. 3. Quantification of immune subpopulations in the inflamed skin. (*A*) $CD11b^+Ly6G^+$ neutrophils infiltrate the skin by 3 h after onset of inflammation after CFA injection and incision, are found in the CFA-injected skin at chronic stages (up to 14 d), and return to baseline levels by 7 d after incision. (*B*) $CD11b^+Ly6G^-$ myeloid cells can be separated into three populations based on Ly6C expression, with $Ly6C^{low}$ myeloid cells constituting the bulk of these cells in the naïve animal. $CD11b^+Ly6G^-Ly6C^{low}$ cells show a biphasic response after CFA injection, peaking at 24 h and again at 14 d, whereas they make up the majority of cells between 3 and 10 d after plantar incision. $CD11b^+Ly6G^-Ly6C^{hi}$ cells, on the contrary, are the most prominent cell type at >3 d after CFA injection and are mostly present in the skin between 24 h and 3 d after incision. $Ly6C^{med}$ myeloid cells follow a pattern similar to that of $Ly6C^{low}$ cells after CFA injection, but have the same recruitment pattern as $Ly6C^{hi}$ cells after incision. (*C*) $CD45^+CD11b^-TCR\beta^+$ T cells show infiltration into the skin from 7 d in both models of peripheral inflammation. (*D* and *E*) Quantification of flow cytometry analysis after CFA injection and plantar incision (n = 3–4 per group per time point). Time point not listed on graphs: 3 h. Graphs show means ± SEM.

controls. We first confirmed the absence of $TCR\beta^+$ T cells in the spleens of naïve $TCR\beta^{-/-}$ (TCRβ-KO) and $TCR\beta^{+/+}$ (TCRβ-WT) littermates, where these cells are usually plentiful (Fig. S2*A*). The TCRβ-KO mice showed no difference in thermal or mechanical hypersensitivity relative to TCRβ-WT mice following intraplantar CFA injection (Fig. S1 *B* and *C*) or plantar incision (Fig. S2 *D* and *E*), leading to our conclusion that T cells do not contribute to acute inflammatory pain. As mechanical and thermal hypersensitivity occur relatively early after inflammation (within 24 h), and T cells enter the tissue much later (>7 d) in both models, it is not surprising that these cells would have little if any contribution to pain outcomes in these models that are biased to innate immunity.

$Ly6G^+$ Neutrophils Do Not Contribute to Inflammatory Pain. To assess the role of neutrophils, which were a major subset of inflammatory cells present early in both models, we depleted these cells by using anti-Gr1 antibody and compared them vs. isotype control and saline solution-treated animals (29). Flow cytometry was carried out at the peak of neutrophil infiltration in the skin (24 h after onset of inflammation) to confirm their depletion after treatment with the anti-Gr1 antibody. We found a significant reduction in neutrophils after CFA injection (Fig. 5*A*) relative to the isotype control, whereas monocytes/Mø were unaffected (Fig. S3*A*). Neutrophil depletion did not result in significant changes in thermal or mechanical hypersensitivity at any time point over the 14-d duration of the study relative to IgG- or saline solution-treated mice (Fig. 5 *B* and *C*). Elimination of neutrophils for plantar incision was performed by using the aforementioned protocol and confirmed by flow cytometry (Fig. 5*D*), and did not alter monocyte/Mø populations (Fig. S3*B*). There were no changes in thermal or mechanical hypersensitivity in the absence of neutrophils relative to control IgG-treated mice or those treated with saline solution (Fig. 5 *E* and *F*), indicating minimal contribution of these cells to the inflammatory pain phenotype. The IgG isotype control did not affect behavior outcomes relative to saline solution-treated controls in either model of inflammatory pain.

Depletion of $CD11b^+Ly6G^-$ Myeloid Cells Alters Mechanical Hypersensitivity. To produce a specific depletion of $CD11b^+Ly6G^-$ myeloid cells, the largest population of infiltrating immune cells in

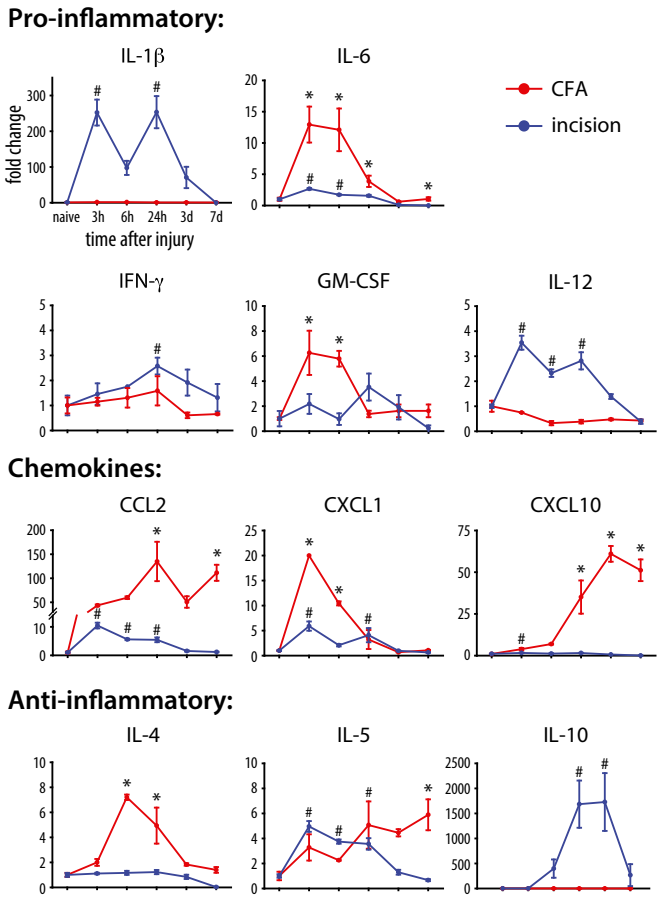

Fig. 4. Multiplex cytokine/chemokine analysis of the inflamed skin reveals distinct molecular inflammatory outcomes after CFA injection and incisional wound. Proteins were analyzed at various time points after onset of inflammation, and are plotted as fold change relative to naïve levels. Only proteins showing significant change over time ($P < 0.05$, one-way RM-ANOVA) are included [$*P < 0.05$ (incision) and $^{\#}P < 0.05$ (CFA), one-way RM-ANOVA with post hoc Bonferroni test for multiple comparisons vs. naïve time point; $n = 3$–4 per group per time point]. Graphs show means ± SEM.

both models of inflammatory pain, we treated CD11b-TK transgenic mice with the nucleoside analog ganciclovir (GCV). The myeloid-specific gene *CD11b* in these mice drives a mutant form of the suicidal Herpes simplex virus 1 thymidine kinase gene (*HSV1-TK*$^{mt\text{-}30}$), and HSV1-TK$^{mt\text{-}30}$ phosphorylates GCV to inhibit DNA synthesis (30, 31), ablating all proliferating transgene positive cells. We found that this treatment resulted in a specific loss of proliferating CD11b^{+}Ly6G^{-} myeloid cells, but not of CD11b^{+}Ly6G^{+} neutrophils (Fig. S4). Proliferating CD11b^{+}Ly6G^{-} myeloid cells were depleted in CFA-injected mice by intraplantar injection of GCV. In the incision group GCV was administered by intraplantar (local) and i.p. (systemic) injection. FACS analysis of CFA-treated mice treated systemically with GCV at the standard dose showed no change in the myeloid cell population at 24 h, and higher doses of GCV were toxic.

Following elimination of CD11b^{+}Ly6G^{-} cells, no significant difference in thermal latency was observed following CFA injection or incision relative to the control groups (Fig. 6 *B* and *E*). In CFA-injected mice, depletion of CD11b^{+}Ly6G^{-} cells reduced mechanical sensitivity relative to all other groups [$P \leq 0.036$, two-way repeated-measures (RM)-ANOVA with post hoc Tukey test]. The effect, however, was limited to the early phase of inflammation (days 1 and 2; Fig. 6*C*). Strikingly, depletion of CD11b^{+}Ly6G^{-} cells in CD11b-TK mice after i.p. treatment with GCV produced a marked elevation in mechanical thresholds over the entire time course after plantar incisional wound, with the myeloid cell-depleted mice showing significantly attenuated hypersensitivity compared with the control groups (Fig. 6*F*). The depleted mice showed no difference in mechanical threshold from their preinjury baseline values from the 24-h time point until the end of the study at 7 d, in contrast to the sustained reduced thresholds in mice with intact myeloid cell populations. Controls for the GCV injection and *CD11b-TK* gene did not show any effect in the behavioral measures. Depletion of proliferating CD11b^{+}Ly6G^{-} myeloid cells by intraplantar injection of GCV after incision (Fig. 6*G*) showed a significant, albeit less robust, effect on mechanical hypersensitivity (Fig. 6 *H* and *I*) that could have resulted from leakage of the GCV from the wound site. These data suggest that proliferating CD11b^{+}Ly6G^{-} myeloid cells are necessary for the mechanical hypersensitivity that follows incisional wound-induced inflammation.

We next used a second myeloid cell targeting strategy to complement the CD11b-TK data using the *CCR2* KO mouse to prevent recruitment of inflammatory monocytes into the hind paw in the incisional wound model. CCR2 is a chemokine receptor required for the infiltration of Ly6C^{+} monocytes into inflamed tissues in response to the chemotactic cytokine CCL2, and *CCR2*$^{-/-}$ mice have been used extensively to study the role of inflammatory monocytes and Mø in various injury and disease models (e.g., refs. 32–34). This mouse line has also been used to study neuropathic pain, which it reduced, and CFA-induced inflammatory pain, in which it had no effect (35), but has not been used to examine the pain response after incisional wound. KO and littermate WT controls were assessed for immune cell recruitment into the hind paw (Fig. 6*J*). We found a significant increase in neutrophils at 24 h, but not at 3 d, and a reduction in Ly6C^{hi} and Ly6C^{med} myeloid cells; the Ly6C^{low} subset displayed a much smaller reduction at 24 h than at 3 d (Fig. S4). These results are in agreement with other studies assessing the recruitment of myeloid cells into inflamed tissues (36–38). The mice were then assessed for thermal and mechanical hypersensitivity after plantar

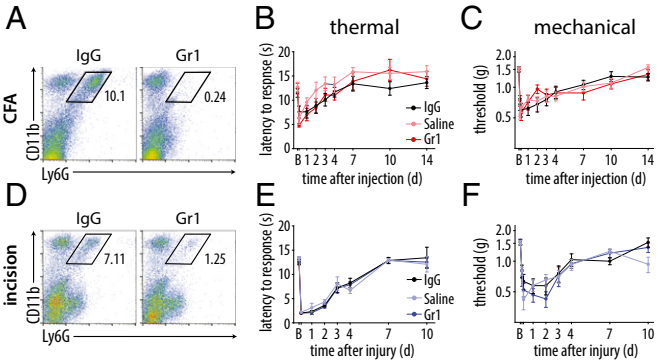

Fig. 5. Neutrophils do not control CFA- or incisional wound-mediated inflammatory hypersensitivity. (*A*) Depletion of neutrophils using the Gr1 antibody was confirmed 24 h after CFA injection by flow cytometry, compared with IgG control antibody ($n = 3$–4 per group). (*B* and *C*) Thermal ($P = 0.813$) and mechanical ($P = 0.258$) hypersensitivity were not altered after intraplantar CFA injection in neutrophil-depleted mice relative to IgG- and saline solution-treated controls ($n = 10$–12 per group). (*D*) Depletion of neutrophils using the Gr1 antibody was confirmed 24 h after plantar incision by flow cytometry, compared with IgG control antibody ($n = 3$–4 per group). (*E* and *F*) Thermal ($P = 0.809$) and mechanical ($P = 0.407$) hypersensitivity were not altered after plantar incision in Gr1-treated mice relative to IgG- or saline solution-treated controls ($n = 11$ per group). *P* values were calculated using two-way RM-ANOVA with post hoc Tukey test. Time points not listed: *B* and *E*, 4 h; *C* and *F*, 3 h and 6 h. Graphs show means ± SEM.

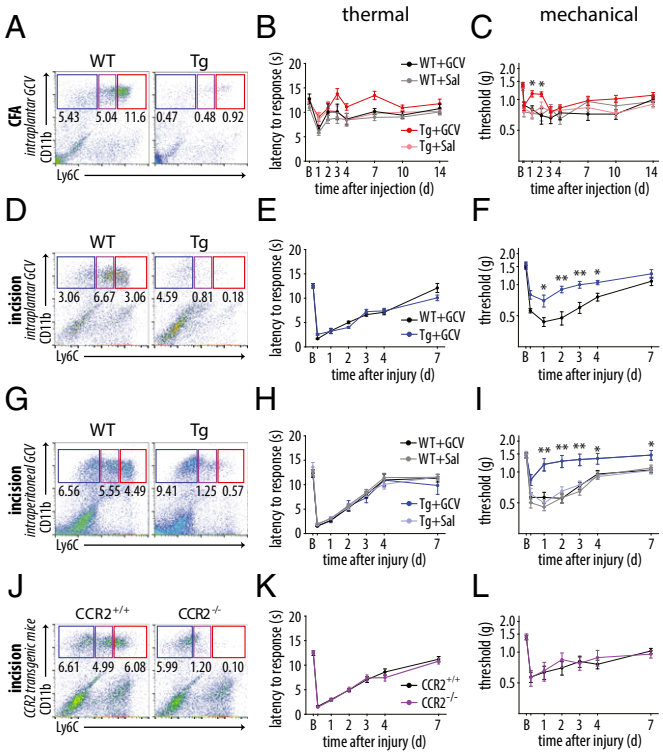

Fig. 6. Proliferating CD11b$^+$Ly6G$^-$ myeloid cells control mechanical hypersensitivity after incisional wound. (*A*) Depletion of nonneutrophil myeloid cells was confirmed 24 h after CFA injection by flow cytometry in CD11b-TK and littermate control mice treated with GCV (n = 3–4 per group). (*B*) Thermal hypersensitivity was not altered after CFA injection in Mø-depleted mice (P = 0.453; n = 9–16 per group). (*C*) Mechanical hypersensitivity was significantly different between depleted mice and the three control groups (P = 0.034), but the effect was significant only at days 1 and 2 after injection (n = 9–16 per group). (*D*) Flow cytometry confirmed depletion of CD11b$^+$Ly6G$^-$ myeloid cells after local injection of GCV in the hind paw after incision (n = 5 per group). (*E*) Thermal hypersensitivity was unaltered between WT and CD11b-TK littermates (P = 0.577; n = 8–10 per group). (*F*) Mechanical hypersensitivity was significantly attenuated in CD11b-TK mice relative to littermates treated with GCV (P < 0.001; n = 8–10 per group). (*G*) Flow cytometry confirmed depletion of myeloid cells in the skin of CD11b-TK mice, relative to WT controls, treated with GCV systemically (n = 3–4 per group). (*H*) Thermal hypersensitivity was unchanged after depletion of monocytes/Mø (P = 0.993; n = 12–18 per group). (*I*) Mechanical hypersensitivity was reversed in CD11b-TK mice treated with GCV, relative to WT controls, beginning at 24 h, with the effect maintained until 7 d (P < 0.001; n = 12–18 per group). (*J*) Flow cytometry confirmed absence of Ly6C$^{med/hi}$ myeloid cells in CCR2$^{-/-}$ mice relative to WT littermates (n = 4–5 per group). (*K* and *L*) Neither thermal nor mechanical hypersensitivity were affected in the *CCR2* KO mice relative to littermate controls (P > 0.743; n = 9–15 per group; **P< 0.001 and *P < 0.05, two-way RM-ANOVA with post hoc Tukey test for behavioral analysis). Time points not listed: *C*, 3 h; *E*, *F*, *H*, *I*, *K*, and *L*, 6 h. Graphs show means ± SEM.

incision, but did not exhibit any difference in either modality (Fig. 6 *K* and *L*).

Transcriptional and Multiplex Cytokine Profiling. Transcriptional expression profiling of FACS-purified CD11b$^+$Ly6G$^-$Ly6C^{hi}, Ly6C^{med}, and Ly6C^{low} cells isolated from the hind paw 24 h after the incisional wound, a time point of significant mechanical hypersensitivity, was carried out by microarray analysis to obtain mechanistic insight into their functional and activation states. A total of 8,169 transcripts remained after filtering out transcripts with low expression (39); the transcript with the highest variability among the three subsets of cells was Ly6C2 (σ = 2,318.2). The 50 most variable transcripts across these subsets were identified and ranked by average expression (Fig. 7*A*). We also filtered the 8,169 transcripts further for those with a Gene Ontology biological function that included the search strings "immun* OR inflamm*", further narrowing this list to 304 records. The 50 immune-related transcripts with the greatest variation across the three populations of myeloid cells were identified and sorted by average expression (Fig. 7*B*). This profiling showed similarities across the three cell types in terms of overall expression levels of certain factors, as well as distinct differences that could reflect differences in activation states and function. Average expression values for several cytokine/chemokine transcripts of interest are also presented, including IL-1β, TNF-α, and CCL3 (Fig. 7*C*).

We next carried out a multiplex cytokine analysis of the postincisional wound site (including skin, muscle, and immune cells) in CD11b-TK and littermate controls treated with GCV in an effort to identify potential mechanisms for the behavioral differences observed. Although no significant differences were observed in the analytes examined at 6 h or 24 h after incision, six cytokines showed significant changes at 3 d postinjury (Fig. 7*D* and Table S2). In particular, the antinociceptive cytokine IL-1α (40) was increased at 3 d after the incisional wound and the pronociceptive cytokine IL-1β (41) was reduced in the CD11b-TK mice. IL-1α, IL-1β and CCL2 were also represented among the 8,169 transcripts expressed by nonneutrophil myeloid cells. IL-1α had the highest expression in Ly6C^{med} cells and lowest in the Ly6C^{low} population, and IL-1β and CCL2 had a consistently high expression (>3,000 normalized expression) in all three cell types.

Discussion

We set out to determine whether specific aspects of the immune response may contribute to the inflammatory pain phenotype. Our approach was to first characterize the temporal course of the cellular immune responses to intraplantar CFA (representative of adjuvant/pathogen-based inflammation) and an incisional wound (representative of sterile tissue injury), and we found quite distinct histological and inflammatory phenotypes and changes in behavioral sensitivity between the two models. Immune cell-targeted depletion of T cells or neutrophils produced no effect on mechanical or thermal pain behaviors in either model. A subset of proliferating CD11b$^+$Ly6G$^-$ myeloid cells, on the contrary, were found to be necessary for one major pain outcome—mechanical hypersensitivity—primarily in the incision model.

CFA injection into the hind paw is widely used to study inflammatory pain because of the robust inflammation it evokes, its reproducibility, and its clear pain phenotype. We found that intraplantar CFA induced a quite different type of inflammation than sterile tissue trauma, and may in consequence have limited utility for modeling common clinical inflammatory pains that can arise from trauma, bacterial infection, or autoimmune diseases. The injection site is characterized by the presence of a focal collection of immune cells (a granuloma comprising primarily Mø) that "wall off" the injected oils, as reported before (42). The impaired clearance of heat-killed *Mycobacterium* and/or the mixture of oils used in the emulsion cause a granulomatous pattern of inflammation (43–45) that naturally occurs only in a very limited number of diseases, including tuberculosis, leprosy (20), and chronic gout (46). Human mycobacterial infections (47, 48) are modeled by injection of mineral/paraffin oil or *Mycobacterium tuberculosis* (49–51), the two components of CFA. This would suggest that the CFA model might be most suitable for the specific study of chronic nonresolving granulomatous inflammatory diseases. Intraplantar injection of live and heat-killed *Staphylococcus aureus* also induces acute thermal and mechanical hypersensitivity that are surprisingly independent of the innate immune system in the early phase, and are caused instead by the direct activation of nociceptors (52). These infection models may

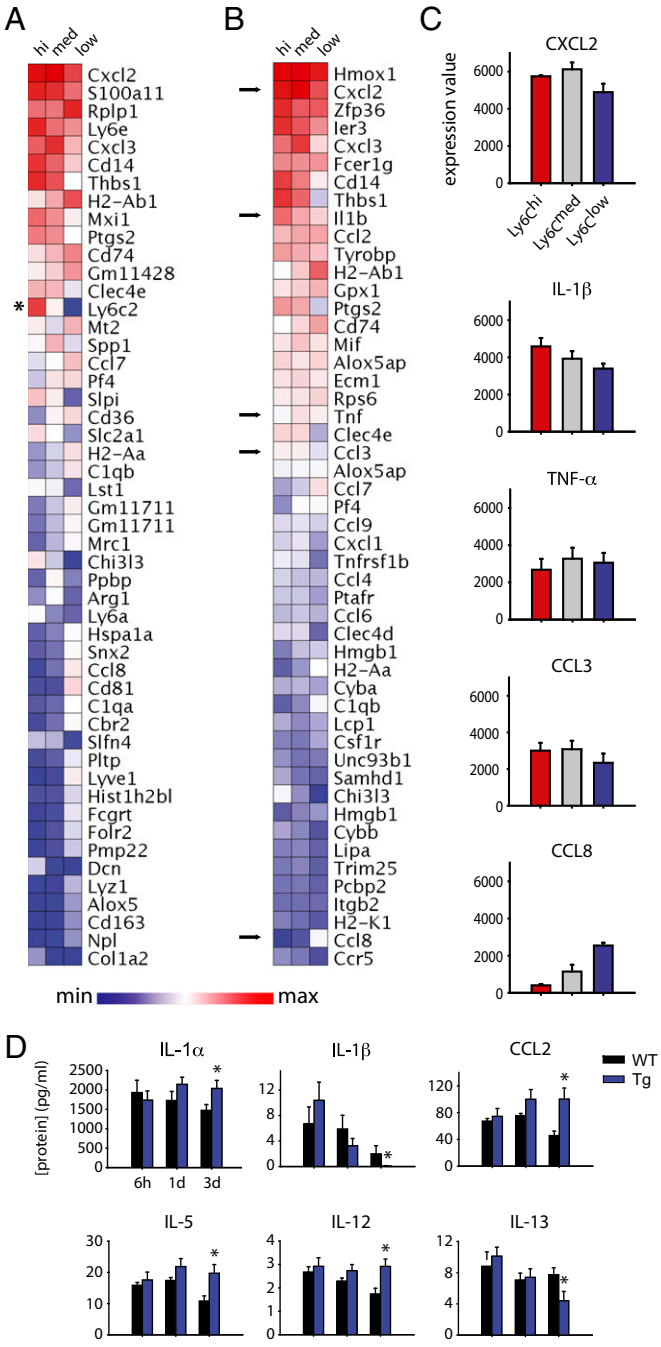

Fig. 7. Distinct transcriptional profiles of CD11b$^+$Ly6G$^-$ myeloid cells and the effects of their depletion on cytokines after incisional wound. CD11b$^+$Ly6G$^-$ myeloid cells were FACS-sorted by Ly6C expression and profiled by using the Affymetrix Mouse Gene ST 2.0 chip. (*A*) Expression patterns of the 50 most variable genes from all expressed transcripts are shown, ranked by overall expression levels, which shows a prevalence of immune-related genes (*Ly6C2, which was used to define the three cell types used in this analysis). (*B*) The 50 most highly expressed immune-related transcripts are shown, ranked in order of average overall expression. (*C*) Expression patterns of five transcripts of interest, identified by arrows in *C*, show similar expression levels of key cytokines across all three populations, and a minority show distinct expression in subsets of cells (n = 3 per cell type). (*D*) Multiplex cytokine analysis of the inflamed hind paw reveals a dysregulated inflammatory after incisional wound in CD11b-TK (Tg) and WT littermate controls treated with GCV systemically (n = 3–4 per group per time point; *$P < 0.05$, one-way RM-ANOVA with post hoc Tukey test for cytokine analysis).

have greater utility than CFA in the study of the pain associated with bacterial pathogens.

Despite being a major infiltrating immune cell type in both models, neutrophils surprisingly did not contribute to thermal or mechanical hypersensitivity after CFA injection or incisional wound. Neutrophils secrete many proinflammatory mediators but also produce opioid peptides that might reduce pain. This dichotomy is evident in the literature, with studies showing that these cells can increase (53–55) or decrease (56, 57) hypersensitivity, whereas others have shown no effect (58, 59) in various models of inflammatory pain. Our results suggest a lack of any major contribution for these cells to pain, at least under our conditions and in other models in which clear depletion was demonstrated. Two studies (54, 60) used a similar antibody-mediated neutrophil depletion paradigm in an incisional wound. Sahbaie et al. (54) found only a minor effect in thermal latency and no change in mechanical threshold. Carreira et al., meanwhile, saw a dramatic reduction in mechanical hypersensitivity with antibody treatment, but this could have been a result of i.v. delivery of the antibody as well as timing of treatment (60). Many of these studies used myeloperoxidase activity as a surrogate for neutrophil infiltration, even though flow cytometry provides a more accurate picture of the presence/absence of these cells. Intraplantar injection of chemokines has also been used to recruit neutrophils into the hind paw, but this might result in a different activation state of the cells than that caused by CFA or an incisional wound (56, 59).

Our data do not mean that neutrophils are not capable of producing pain, but that they are not required, presumably because other cells are sufficient to drive the phenotype in their absence. The role of neutrophils has been studied extensively in wound healing, and depletion studies using models of tissue injury have similar varied results (61–63). As expected, depletion of circulating T cells that enter the tissue late (≥7 d) after injury had no effect on behavioral outcomes in these two acute pain models whose inflammation in the early phase results from innate immune responses. T lymphocytes have also been studied in wound healing, albeit less extensively. T-cell depletion studies in models of wound healing have produced contradictory results depending on the depletion strategies, species, and mode of injury (64–67).

Nonneutrophil myeloid cells are primarily responsible for the phagocytosis of debris and invading pathogens in incisional wounds, and, although they are not required for tissue repair, they do play important roles in vascularization, fibrosis, and scarring (37, 68, 69). There are, however, relatively few studies examining the effect of myeloid cell depletion in inflammatory pain, and these show contradictory results. One study showed that local depletion of Mø using clodronate liposomes did not alter pain behavior after intraplantar injection of CFA (56), whereas others have reported that systemic depletion of these cells using clodronate liposomes or an α-CCR2 antibody results in an unexpected increase in mechanical and thermal hypersensitivity after intraplantar injection of carrageenan (70) or CFA (71). The mechanisms suggested for the inferred antinociceptive effects for these cells was that they either secrete β-endorphins (71) or act in the dorsal root ganglia and spinal cord to produce antiinflammatory cytokines like IL-10 (70). However, multiple other studies of peripheral nerve injury and diabetic neuropathy have shown, as for incisional pain, that depletion or delayed infiltration of myeloid cells resulted in reduced pain sensitivity (35, 72–75). We show that depletion of CD11b$^+$Ly6G$^-$ cells had a slight and short-lasting effect after CFA injection but resulted in the abrogation of mechanical hypersensitivity in the incision model.

We also observed differences in inflammatory mediator profiles between CFA-injected and incised hind paws. The prototypical inflammatory mediator IL-1β was expressed only after the incisional wound, whereas IL-6 showed dramatically higher expression in the CFA model. Expression of the antiinflammatory

mediator IL-4 was restricted to the early (<24 h) phase of CFA inflammation, whereas IL-10 was expressed only after incisional wound and in its resolution phase (1-3 d). Chemokines showed the highest expression in CFA-injected tissue, suggesting a mechanism for the continued recruitment/activation of immune cells. The profiling also revealed a dysregulation of the cytokine response in the absence of Mø in the incisional model. For example, IL-1β was reduced 3 d postincision in GCV/CD11b-TK mice. As IL-1β is an important contributor to the development of mechanical hypersensitivity (41, 76–78), this may help explain the reduced pain in this situation. Although IL-1α and CCL2 were expressed at high levels in sorted myeloid cells, protein levels increased when these cells were depleted in CD11b-TK/GCV depleted mice, suggesting a compensatory mechanism controlling their expression. Furthermore, IL-5, -12, and -13 were also significantly expressed in the myeloid cell-depleted mice but were not expressed by any of the sorted myeloid cells. These three cytokines are likely expressed by other reactive cells in the injured tissue, including fibroblasts, muscle, and/or other immune cells (e.g., neutrophils, mast cells, and skin-resident Mø). Some cytokines (e.g., interferons) are absorbed by tissue cells soon after release making protein detection difficult.

We interpret our data as indicating an important role for a subset of proliferating nonneutrophilic myeloid cells in the maintenance of mechanical hypersensitivity following sterile tissue injury, but exactly which set and how they do this now needs to be explored. The finding that *CCR2*$^{-/-}$ mice did not exhibit any difference in pain may help identify the cells responsible. Although all subsets of proliferating CD11b^{+} myeloid cells are depleted in the CD11b-TK line, only a subset of these cells fail to be recruited to the site of inflammation in *CCR2*$^{-/-}$ mice. There are several possible explanations for the behavioral differences we observe between CCR2 and CD11b-TK mice. The increased presence of neutrophils in *CCR2*$^{-/-}$ mice might offset the effects of reduced myeloid cell recruitment/depletion at the site of injury through release of neutrophil-derived mediators. Another possibility is that a particular population of CD11b^{+}Ly6G^{-} Ly6C^{med} or Ly6C^{low} myeloid cells are responsible for the changes in mechanical hypersensitivity. Although treatment of CD11b-TK mice with GCV eliminates all proliferating CD11b^{+} cells (including skin-resident and peripheral CD11b^{+} cells), *CCR2* KO only reduces recruitment of CCR2^{+} myeloid cells from the blood into the injured skin. We therefore conclude that one or more subsets of skin-resident CD11b^{+} myeloid cells (e.g., mast cells, epidermal and dermal dendritic cells, Langerhans cells, and natural killer cells) or circulating Ly6C^{med} and/or Ly6C^{low} myeloid cells, which have recently been shown to play an important role in the development of inflammatory disease (79), may be the major cellular drivers of mechanical pain hypersensitivity.

We find that the Ly6C^{low} population expresses many proinflammatory mediators, including IL-1β, TNF-α, and CCL8, and thus cannot be considered equivalent to antiinflammatory Mø, which tend to express high levels of IL-4 and IL-10 and may be contributors to the pain phenotype. Unfortunately, no tools exist to specifically deplete and/or inhibit infiltration of Ly6C^{low} or Ly6C^{med} cells. Skin-resident immune cells can drive inflammation in the skin by interacting directly with nociceptors (80, 81), but were not definitively extracted by our FACS protocol. Furthermore, fibroblasts, keratinocytes, muscle, and other cells may also be activated by the inflammatory milieu (82, 83) to secrete factors that activate or sensitize nociceptors (84, 85).

The specific cellular and molecular cues responsible for mechanical and thermal hypersensitivity remain to be elucidated. Nevertheless, our finding of a nonredundant myeloid cell-based mechanism for inflammatory mechanical hypersensitivity is intriguing, especially because there is a large clinical need for control of this pain postsurgery and in arthritis. Which factors produced by which Mø-like cell generate mechanical hypersensitivity, and, if it is the specific result of changes in mechanotransducer channels or a consequence of increased membrane excitability, now need to be studied. The immune responses responsible for the development and maintenance of inflammatory pain are complex and diverse, and study of inflammatory pain needs detailed specification of the precise kind, location, and time of the underlying inflammation. Treatment of inflammatory pain may need to be tailored to specific types of inflammation and their temporal phase, as these will determine the nature, number, and activation of infiltrating immune cells and their collective effects on the pain phenotype. Nevertheless, our findings point to the potential advantages of targeting selective myeloid cell populations for reducing mechanical pain hypersensitivity.

Methods

Experimental Animals and Surgery. All work was performed in 8–12-wk-old male mice housed in a light- and temperature-controlled room. C57BL/6J mice (Jackson Labs) were used for most experiments except where noted. T-cell–deficient B6.129P2-*Tcrb*^{tm1Mom} *Tcrd*$^{tm1Mom/J}$ mice (Jackson Labs) were backcrossed to C57BL/6J to generate WT and TCRβ$^{-/-}$αβ T-cell KO littermates (86). CD11b-TK$^{mt\text{-}30}$ mice (generated and provided by Jean-Pierre Julien, Université Laval, Québec, QC, Canada) were bred as previously described (87) with C57BL/6J mice to generate both WT and transgenic (CD11b-TK) littermates. CCR2$^{-/-}$ B6.129S4-*Ccr2*^{tm1Ifc}/J mice (Jackson Labs) were backcrossed to C57BL/6J to generate WT (CCR2$^{+/+}$) and KO (CCR2$^{-/-}$) littermates. The institutional animal care and use committee of Boston Children's Hospital approved all animal care and procedures.

Pathogen-based peripheral inflammation was induced by intraplantar injection of 20 μL of CFA (Sigma-Aldrich) into the left hind paw of conscious mice with a 26-gauge Hamilton microsyringe. Sterile tissue injury-based peripheral inflammation was induced by using a deep plantar incision of the left hind paw using a modification of a technique previously described (16). Briefly, mice were anesthetized with 2% (vol/vol) isoflurane (maintained at 1.5% during surgery) and the left hind paw sterilized with 10% (wt/vol) povidone-iodine and 100% ethanol. The skin and underlying muscle were cut along the midline by using a number-11 scalpel from the base of the heel to the first walking pad, and the overlying skin was sutured at two sites using 6-0 sutures (Ethilon). All surgeries and injections were carried out blinded to genotype and/or treatment.

Histology. Mice were deeply anesthetized and euthanized by transcardial perfusion with 4% paraformaldehyde in 0.1 M phosphate buffer. The hind paw including skin and underlying muscles was removed, postfixed for 1 h, and cryoprotected in 30% sucrose in 0.1 M phosphate buffer for 48 h. Serial cryostat cross sections (14 μm thickness) were obtained for histological analysis. Sections were stained with H&E as previously described (88).

Flow Cytometry. Analysis of immune cell infiltration/recruitment was carried out as previously described (52). Briefly, paw tissue was minced and digested in a mixture of 1 mg/mL collagenase A and 2.4 U/mL Dispase II (Roche Applied Sciences) in Hepes-buffered saline solution for 90 min. After digestion, cells were triturated by pipette, washed with HBSS and 0.5% BSA, and filtered through a 70-μm mesh, and the cells were blocked by using rat anti-CD16/CD32 (Fc block; 1:10 hybridoma supernatant) on ice for 5 min. To analyze the presence of T cells, spleens were removed and passed through a 70-μm mesh and blocked by using Fc block. The cells were then incubated with mixtures of the following antibodies (all from BioLegend; 1:200 unless noted): (*i*) anti–CD11b-PE (1:1,000), anti–Ly6G-APC, and anti–Ly6C-FITC, or (*ii*) anti–CD11b-PE (1:1,000), anti–CD45-APC, and anti–TCRβ-FITC. Flow cytometry was conducted on a FACSCalibur machine (Becton Dickinson) equipped with argon and helium-neon laser. Flow cytometry data were analyzed by using FlowJo software (TreeStar). For microarrays, CD11b^{+}Ly6G^{-} myeloid cells were gated by Ly6C expression and sorted directly into QIAzol (Qiagen). To minimize technical variability, all cells were sorted on the same day for microarray analysis.

Immune Cell Depletion Strategies. Male C57BL/6J mice were given i.p. injections of a low dose (125 μg dissolved in a total of 200 μL saline solution) of rat anti-mouse Ly6G/Gr1 antibody (clone RB6-8C5; BioXCell) to deplete circulating neutrophils starting 24 h before onset of inflammation and then every 3 d thereafter, a protocol previously shown to deplete neutrophils without altering the Mø population (29). An equal amount and volume of the isotype control antibody rat anti-IgG2b (BioXCell; dissolved in saline solution)

or saline solution (Sigma) were used as controls. Mø were depleted by using CD11b-TK mice upon administration of GCV. All mice received an i.p. injection of GCV (100 mg/kg) 12 h before onset of inflammation. Mice injected with CFA received intraplantar injections of 100 μg GCV (in 10 μL saline solution); those with incisions received either intraplantar injections (as in CFA) or i.p. injections of 100 mg/kg GCV to deplete $CD11b^+$ cells. Injections were given every 12 h to ensure continuous depletion of the cells. Controls groups included WT littermate controls injected with GCV or saline solution and CD11b-TK mice injected with saline solution. Transgenic mice homozygous for a targeted mutation of the TCRβ locus are deficient in the αβ T-cell receptor, resulting in a >90% loss of circulating T cells (86). Confirmation of immune cell depletion by flow cytometry was done at least in triplicate.

Thermal and Mechanical Hypersensitivity. Mechanical threshold was measured using von Frey monofilaments (Ugo Basile), and defined as the minimum filament weight needed to elicit at least five responses (fast paw withdrawal, flinching, licking/biting of the stimulated paw) over a total of 10 stimulations. The Plantar Analgesia Meter (Hargreaves's test; IITC Life Science) was used to assess response latency to a radiant heat stimulus. Mice were assessed for thermal and mechanical hypersensitivity as previously described (19), with minor changes. Briefly, mice were habituated for 1 h daily in individual compartments for each behavior assay. Three baseline measurements were then taken on separate days for mechanical threshold and thermal latency to response and averaged. One value was taken per mouse for mechanical threshold and an average of three values was taken per mouse for thermal latency at each time point used. All behavioral experiments were carried out using at least two independent cohorts of mice.

Microarray Analysis. Flow cytometry was used to purify $CD11b^+Ly6G^-$ myeloid cells by Ly6C expression. Cells were sorted directly into QIAzol, and RNA extracted by sequential extraction and purification using the RNEasy Lipid Tissue Mini kit (Qiagen) with on column DNA digestion according to the manufacturer's instructions. RNA quality was determined by an Agilent 2100 Bioanalyzer using the Pico chip (Agilent). Samples with RNA integrity number (RIN) > 7 were used for analysis. RNA was amplified into cDNA by using the Applause WT-Amp ST System expression kit (NuGEN), with Poly-A controls from the GeneChip Eukaryotic Poly-A RNA control kit (Affymetrix). The Affymetrix GeneChip WT Terminal labeling kit was used for fragmentation and biotin labeling. Affymetrix GeneChip Hybridization control kit and the Affymetrix GeneChip Hybridization, wash, stain kit was used to hybridize samples to Affymetrix Mouse Gene ST 2.0 GeneChips. Fluidics were performed on the Affymetrix GeneChip Fluidics Station 450, and scanned by using a GeneChip Scanner 7G (Affymetrix). Microarray work was conducted at the Boston Children's Hospital Intellectual & Developmental Disabilities Research Center (IDDRC) Molecular Genetics Core. For bioinformatics analysis, Affymetrix CEL files were normalized using the robust multiarray average algorithm with quantile normalization, background correction, and median scaling. The microarray data has been deposited in the Gene Expression Omnibus database under accession number GSE73667. Transcripts were filtered for mean expression values >100 in any one population (39) and sorted by variability across the three populations of cells. Heat maps were generated by using the GenePattern platform (Broad Institute). Keyword searches for immune-related transcripts "immun* OR inflamm*" were carried out using Excel (Microsoft).

Multiplex Cytokine Assay. Hind paws, including skin and underlying muscle, were removed and homogenized on ice in PBS solution with protease and phosphatase inhibitors (Roche). Tissue samples were then analyzed for cytokines/chemokines by using Multiplex MAP Mouse Cytokine/Chemokine Magnetic Bead (EMD Millipore) and/or Novex Cytokine Magnetic Bead (Invitrogen) panels. Cytokine concentrations calculated using available standards and change in expression were calculated as fold change vs. naïve controls.

Statistical Analysis. All statistical analyses were carried out by using the SigmaStat/SigmaPlot software packages (Systat Software). A *t* test was used for direct comparisons between two groups. For multiple comparisons within one group, one-way ANOVA or one-way RM-ANOVA were used, whereas two-way RM-ANOVA was used for multiple comparisons between two or more groups. Post hoc tests used included the Bonferroni *t* test for multiple comparisons vs. control and Tukey's *t* test for multiple comparisons.

ACKNOWLEDGMENTS. The authors thank E. Cobos del Moral, A. Trevino, V. Robson, O. Babanyi, and H. Patoski for technical help and N. Andrews and B. Singh for comments. This work was supported by National Institutes of Health (NIH) Grant 5R37NS039518-13 (to C.J.W.), Canadian Institutes of Health Research (CIHR) and Fonds de recherche en santé du Québec (FRSQ) fellowships (to N.G.), and an NIH fellowship (to I.M.C.).

1. Kidd BL, Urban LA (2001) Mechanisms of inflammatory pain. *Br J Anaesth* 87(1):3–11.
2. Woolf CJ, Ma Q (2007) Nociceptors–noxious stimulus detectors. *Neuron* 55(3):353–364.
3. Verri WA, Jr, et al. (2006) Hypernociceptive role of cytokines and chemokines: targets for analgesic drug development? *Pharmacol Ther* 112(1):116–138.
4. Miller RJ, Jung H, Bhangoo SK, White FA (2009) Cytokine and chemokine regulation of sensory neuron function. *Handbook Exp Pharmacol* 194:417–449.
5. Rittner HL, Brack A, Stein C (2008) The other side of the medal: how chemokines promote analgesia. *Neurosci Lett* 437(3):203–208.
6. McMahon SB, Bennett DLH, Bevan S (2006) Inflammatory mediators and modulators of pain. Wall and Melzack's Textbook of Pain (Elsevier/Churchill Livingstone, Philadelphia), Vol 5, pp 49–72.
7. Grace PM, Hutchinson MR, Maier SF, Watkins LR (2014) Pathological pain and the neuroimmune interface. *Nat Rev Immunol* 14(4):217–231.
8. Kolaczkowska E, Kubes P (2013) Neutrophil recruitment and function in health and inflammation. *Nat Rev Immunol* 13(3):159–175.
9. Mahdavian Delavary B, van der Veer WM, van Egmond M, Niessen FB, Beelen RH (2011) Macrophages in skin injury and repair. *Immunobiology* 216(7):753–762.
10. Duffield JS, et al. (2005) Selective depletion of macrophages reveals distinct, opposing roles during liver injury and repair. *J Clin Invest* 115(1):56–65.
11. Serhan CN, Savill J (2005) Resolution of inflammation: the beginning programs the end. *Nat Immunol* 6(12):1191–1197.
12. Hoebe K, Janssen E, Beutler B (2004) The interface between innate and adaptive immunity. *Nat Immunol* 5(10):971–974.
13. Djouhri L, Koutsikou S, Fang X, McMullan S, Lawson SN (2006) Spontaneous pain, both neuropathic and inflammatory, is related to frequency of spontaneous firing in intact C-fiber nociceptors. *J Neurosci* 26(4):1281–1292.
14. Hurley RW, Hammond DL (2000) The analgesic effects of supraspinal mu and delta opioid receptor agonists are potentiated during persistent inflammation. *J Neurosci* 20(3):1249–1259.
15. Ren K, Dubner R (1996) Enhanced descending modulation of nociception in rats with persistent hindpaw inflammation. *J Neurophysiol* 76(5):3025–3037.
16. Brennan TJ, Vandermeulen EP, Gebhart GF (1996) Characterization of a rat model of incisional pain. *Pain* 64(3):493–501.
17. Banik RK, Woo YC, Park SS, Brennan TJ (2006) Strain and sex influence on pain sensitivity after plantar incision in the mouse. *Anesthesiology* 105(6):1246–1253.
18. Pogatzki EM, Raja SN (2003) A mouse model of incisional pain. *Anesthesiology* 99(4): 1023–1027.
19. Cobos EJ, et al. (2012) Inflammation-induced decrease in voluntary wheel running in mice: A nonreflexive test for evaluating inflammatory pain and analgesia. *Pain* 153(4): 876–884.
20. Kunkel SL, Chensue SW, Strieter RM, Lynch JP, Remick DG (1989) Cellular and molecular aspects of granulomatous inflammation. *Am J Respir Cell Mol Biol* 1(6):439–447.
21. Almarestani L, Fitzcharles MA, Bennett GJ, Ribeiro-da-Silva A (2011) Imaging studies in Freund's complete adjuvant model of regional polyarthritis, a model suitable for the study of pain mechanisms, in the rat. *Arthritis Rheum* 63(6):1573–1581.
22. Marks F, Fürstenberger G (1993) Proliferative responses of the skin to external stimuli. *Environ Health Perspect* 101(Suppl 5):95–101.
23. Odland G, Ross R (1968) Human wound repair. I. Epidermal regeneration. *J Cell Biol* 39(1):135–151.
24. Shi C, Pamer EG (2011) Monocyte recruitment during infection and inflammation. *Nat Rev Immunol* 11(11):762–774.
25. Yang J, Zhang L, Yu C, Yang XF, Wang H (2014) Monocyte and macrophage differentiation: Circulation inflammatory monocyte as biomarker for inflammatory diseases. *Biomark Res* 2(1):1.
26. Clements M, et al. (2015) Differential Ly6C expression after renal ischemia-reperfusion identifies unique macrophage populations. *J Am Soc Nephrol*, 10.1681/ASN.2014111138.
27. Ginhoux F, Jung S (2014) Monocytes and macrophages: Developmental pathways and tissue homeostasis. *Nat Rev Immunol* 14(6):392–404.
28. Ji RR, Xu ZZ, Gao YJ (2014) Emerging targets in neuroinflammation-driven chronic pain. *Nat Rev Drug Discov* 13(7):533–548.
29. Kim JV, Kang SS, Dustin ML, McGavern DB (2009) Myelomonocytic cell recruitment causes fatal CNS vascular injury during acute viral meningitis. *Nature* 457(7226):191–195.
30. Gowing G, Vallières L, Julien JP (2006) Mouse model for ablation of proliferating microglia in acute CNS injuries. *Glia* 53(3):331–337.
31. Barrette B, et al. (2008) Requirement of myeloid cells for axon regeneration. *J Neurosci* 28(38):9363–9376.
32. Boring L, et al. (1997) Impaired monocyte migration and reduced type 1 (Th1) cytokine responses in C-C chemokine receptor 2 knockout mice. *J Clin Invest* 100(10): 2552–2561.
33. Izikson L, Klein RS, Charo IF, Weiner HL, Luster AD (2000) Resistance to experimental autoimmune encephalomyelitis in mice lacking the CC chemokine receptor (CCR)2. *J Exp Med* 192(7):1075–1080.
34. Iijima N, Mattei LM, Iwasaki A (2011) Recruited inflammatory monocytes stimulate antiviral Th1 immunity in infected tissue. *Proc Natl Acad Sci USA* 108(1):284–289.

35. Abbadie C, et al. (2003) Impaired neuropathic pain responses in mice lacking the chemokine receptor CCR2. *Proc Natl Acad Sci USA* 100(13):7947–7952.
36. Lu H, et al. (2011) Macrophages recruited via CCR2 produce insulin-like growth factor-1 to repair acute skeletal muscle injury. FASEB *J* 25(1):358–369.
37. Willenborg S, et al. (2012) CCR2 recruits an inflammatory macrophage subpopulation critical for angiogenesis in tissue repair. *Blood* 120(3):613–625.
38. Zigmond E, et al. (2012) Ly6C hi monocytes in the inflamed colon give rise to pro-inflammatory effector cells and migratory antigen-presenting cells. *Immunity* 37(6): 1076–1090.
39. Mingueneau M, et al.; Immunological Genome Consortium (2013) The transcriptional landscape of αβ T cell differentiation. *Nat Immunol* 14(6):619–632.
40. Mika J, et al. (2008) Interleukin-1 alpha has antiallodynic and antihyperalgesic activities in a rat neuropathic pain model. *Pain* 138(3):587–597.
41. Binshtok AM, et al. (2008) Nociceptors are interleukin-1beta sensors. *J Neurosci* 28(52):14062–14073.
42. Wiedemann F, et al. (1991) Histopathological studies on the local reactions induced by complete Freund's adjuvant (CFA), bacterial lipopolysaccharide (LPS), and synthetic lipopeptide (P3C) conjugates. *J Pathol* 164(3):265–271.
43. Broderson JR (1989) A retrospective review of lesions associated with the use of Freund's adjuvant. *Lab Anim Sci* 39(5):400–405.
44. Del Rosario RN, Barr RJ, Graham BS, Kaneshiro S (2005) Exogenous and endogenous cutaneous anomalies and curiosities. *Am J Dermatopathol* 27(3):259–267.
45. Shah NM, Mangat GK, Balakrishnan C, Buch VI, Joshi VR (2001) Accidental self-injection with Freund's complete adjuvant. *J Assoc Physicians India* 49:366–368.
46. Dalbeth N, et al. (2010) Cellular characterization of the gouty tophus: A quantitative analysis. *Arthritis Rheum* 62(5):1549–1556.
47. Stump PR, et al. (2004) Neuropathic pain in leprosy patients. *Int J Leprosy Other Mycobact Dis* 72(2):134–138.
48. Pigrau-Serrallach C, Rodriguez-Pardo D (2013) Bone and joint tuberculosis. *Eur Spine J* 22(suppl 4):556–566.
49. Granger DL, Yamamoto KI, Ribi E (1976) Delayed hypersensitivity and granulomatous response after immunization with protein antigens associated with a mycobacterial glycolipid and oil droplets. *J Immunol* 116(2):482–488.
50. Billiau A, Matthys P (2001) Modes of action of Freund's adjuvants in experimental models of autoimmune diseases. *J Leukoc Biol* 70(6):849–860.
51. Cosma CL, Humbert O, Ramakrishnan L (2004) Superinfecting mycobacteria home to established tuberculous granulomas. *Nat Immunol* 5(8):828–835.
52. Chiu IM, et al. (2013) Bacteria activate sensory neurons that modulate pain and inflammation. *Nature* 501(7465):52–57.
53. Cunha TM, et al. (2008) Crucial role of neutrophils in the development of mechanical inflammatory hypernociception. *J Leukoc Biol* 83(4):824–832.
54. Sahbaie P, Li X, Shi X, Clark JD (2012) Roles of Gr-1+ leukocytes in postincisional nociceptive sensitization and inflammation. *Anesthesiology* 117(3):602–612.
55. Lavich TR, et al. (2006) Neutrophil infiltration is implicated in the sustained thermal hyperalgesic response evoked by allergen provocation in actively sensitized rats. *Pain* 125(1-2):180–187.
56. Brack A, et al. (2004) Control of inflammatory pain by chemokine-mediated recruitment of opioid-containing polymorphonuclear cells. *Pain* 112(3):229–238.
57. Rittner HL, et al. (2009) Antinociception by neutrophil-derived opioid peptides in noninflamed tissue–role of hypertonicity and the perineurium. *Brain Behav Immun* 23(4):548–557.
58. Suo J, et al. (2014) Neutrophils mediate edema formation but not mechanical allodynia during zymosan-induced inflammation. *J Leukoc Biol* 96(1):133–142.
59. Rittner HL, et al. (2006) Selective local PMN recruitment by CXCL1 or CXCL2/3 injection does not cause inflammatory pain. *J Leukoc Biol* 79(5):1022–1032.
60. Carreira EU, et al. (2013) Neutrophils recruited by CXCR1/2 signalling mediate post-incisional pain. *Eur J Pain* 17(5):654–663.
61. Nishio N, Okawa Y, Sakurai H, Isobe K (2008) Neutrophil depletion delays wound repair in aged mice. *Age (Dordr)* 30(1):11–19.
62. Simpson DM, Ross R (1972) The neutrophilic leukocyte in wound repair a study with antineutrophil serum. *J Clin Invest* 51(8):2009–2023.
63. Dovi JV, He LK, DiPietro LA (2003) Accelerated wound closure in neutrophil-depleted mice. *J LeukocBiol* 73(4):448–455.
64. Peterson JM, Barbul A, Breslin RJ, Wasserkrug HL, Efron G (1987) Significance of T-lymphocytes in wound healing. *Surgery* 102(2):300–305.
65. Chen L, Mehta ND, Zhao Y, DiPietro LA (2014) Absence of CD4 or CD8 lymphocytes changes infiltration of inflammatory cells and profiles of cytokine expression in skin wounds, but does not impair healing. *Exp Dermatol* 23(3):189–194.
66. Davis PA, Corless DJ, Aspinall R, Wastell C (2001) Effect of CD4(+) and CD8(+) cell depletion on wound healing. *Br J Surg* 88(2):298–304.
67. Hofmann U, et al. (2012) Activation of CD4+ T lymphocytes improves wound healing and survival after experimental myocardial infarction in mice. *Circulation* 125(13): 1652–1663.
68. Sunderkötter C, Steinbrink K, Goebeler M, Bhardwaj R, Sorg C (1994) Macrophages and angiogenesis. *J Leukoc Biol* 55(3):410–422.
69. Leibovich SJ, Ross R (1976) A macrophage-dependent factor that stimulates the proliferation of fibroblasts in vitro. *Am J Pathol* 84(3):501–514.
70. Willemen HL, et al. (2014) Monocytes/macrophages control resolution of transient inflammatory pain. *J Pain* 15(5):496–506.
71. Sauer RS, et al. (2014) Toll like receptor (TLR)-4 as a regulator of peripheral endogenous opioid-mediated analgesia in inflammation. *Mol Pain* 10(1):10.
72. Liu T, van Rooijen N, Tracey DJ (2000) Depletion of macrophages reduces axonal degeneration and hyperalgesia following nerve injury. *Pain* 86(1-2):25–32.
73. Mert T, et al. (2009) Macrophage depletion delays progression of neuropathic pain in diabetic animals. *Naunyn Schmiedebergs Arch Pharmacol* 379(5):445–452.
74. Sommer C, Schäfers M (1998) Painful mononeuropathy in C57BL/Wld mice with delayed wallerian degeneration: Differential effects of cytokine production and nerve regeneration on thermal and mechanical hypersensitivity. *Brain Res* 784(1-2):154–162.
75. Myers RR, Heckman HM, Rodriguez M (1996) Reduced hyperalgesia in nerve-injured WLD mice: Relationship to nerve fiber phagocytosis, axonal degeneration, and regeneration in normal mice. *Exp Neurol* 141(1):94–101.
76. Kim MJ, et al. (2014) Differential regulation of peripheral IL-1β-induced mechanical allodynia and thermal hyperalgesia in rats. *Pain* 155(4):723–732.
77. Ferreira SH, Lorenzetti BB, Bristow AF, Poole S (1988) Interleukin-1 beta as a potent hyperalgesic agent antagonized by a tripeptide analogue. *Nature* 334(6184):698–700.
78. Ren K, Torres R (2009) Role of interleukin-1beta during pain and inflammation. *Brain Res Brain Res Rev* 60(1):57–64.
79. Misharin AV, et al. (2014) NonclassicalLy6C(-) monocytes drive the development of inflammatory arthritis in mice. *Cell Reports* 9(2):591–604.
80. Riol-Blanco L, et al. (2014) Nociceptive sensory neurons drive interleukin-23-mediated psoriasiform skin inflammation. *Nature* 510(7503):157–161.
81. Stead RH, et al. (1987) Intestinal mucosal mast cells in normal and nematode-infected rat intestines are in intimate contact with peptidergic nerves. *Proc Natl Acad Sci USA* 84(9):2975–2979.
82. Wilson SR, et al. (2013) The epithelial cell-derived atopic dermatitis cytokine TSLP activates neurons to induce itch. *Cell* 155(2):285–295.
83. Roosterman D, Goerge T, Schneider SW, Bunnett NW, Steinhoff M (2006) Neuronal control of skin function: the skin as a neuroimmunoendocrine organ. *Physiol Rev* 86(4):1309–1379.
84. Radtke C, Vogt PM, Devor M, Kocsis JD (2010) Keratinocytes acting on injured afferents induce extreme neuronal hyperexcitability and chronic pain. *Pain* 148(1):94–102.
85. Pastore S, Mascia F, Girolomoni G (2006) The contribution of keratinocytes to the pathogenesis of atopic dermatitis. *Eur J Dermatol* 16(2):125–131.
86. Mombaerts P, et al. (1992) Mutations in T-cell antigen receptor genes alpha and beta block thymocyte development at different stages. *Nature* 360(6401):225–231.
87. Gowing G, Vallières L, Julien P (2006) Mouse model for ablation of proliferating microglia in acute CNS injuries. *Glia* 53(3):331–337.
88. Ghasemlou N, Kerr BJ, David S (2005) Tissue displacement and impact force are important contributors to outcome after spinal cord contusion injury. *Exp Neurol* 196(1): 9–17.